◆ Human Brain Mapping 30:1444–1456 (2009) ◆

Analysis of Lesions in Patients With Unilateral Tactile Agnosia Using Cytoarchitectonic Probabilistic Maps

Lars Hömke,[1] Katrin Amunts,[1,2,3] Lutz Bönig,[4] Christian Fretz,[5] Ferdinand Binkofski,[6] Karl Zilles,[1,7] and Bruno Weder[4,8]*

[1]*Institute of Neurosciences and Biophysics - Medicine (INB3), Research Centre Jülich, Jülich, Germany*
[2]*Department of Psychiatry and Psychotherapy, RWTH Aachen University, Aachen, Germany*
[3]*JARA, Jülich-Aachen Research Alliance*
[4]*Department of Neurology, Kantonsspital St. Gallen, St. Gallen, Switcherland*
[5]*Institute of Radiology, Kantonsspital St. Gallen, St. Gallen, Switzerland*
[6]*Department of Neurology, University Hospital Schleswig-Holstein, Campus Lübeck, Lübeck, Germany*
[7]*C&O Vogt Institut für Hirnforschung, Heinrich-Heine Universität Düsseldorf, Düsseldorf, Germany*
[8]*University of Bern, Switzerland*

Abstract: We propose a novel methodical approach to lesion analyses involving high-resolution MR images in combination with probabilistic cytoarchitectonic maps. 3D-MR images of the whole brain and the manually segmented lesion mask are spatially normalized to the reference brain of a stereotaxic probabilistic cytoarchitectonic atlas using a multiscale registration algorithm based on an elastic model. The procedure is demonstrated in three patients suffering from aperceptive tactile agnosia of the right hand due to chronic infarction of the left parietal cortex. Patient 1 presents a lesion in areas of the postcentral sulcus, Patient 3 in areas of the superior parietal lobule and adjacent intraparietal sulcus, and Patient 2 lesions in both regions. On the basis of neurobehavioral data, we conjectured degradation of sequential elementary sensory information processing within the postcentral gyrus, impeding texture recognition in Patients 1 and 2, and disturbed kinaesthetic information processing in the posterior parietal lobe, causing degraded shape recognition in the patients 2 and 3. The involvement of Brodmann areas 4a, 4p, 3a, 3b, 1, 2, and areas IP1 and IP2 of the intraparietal sulcus was assessed in terms of the voxel overlap between the spatially transformed lesion masks and the 50%-isocontours of the cytoarchitectonic maps. The disruption of the critical cytoarchitectonic areas and the impaired subfunctions, texture and shape recognition, relate as conjectured above. We conclude that the proposed method represents a promising approach to hypothesis-driven lesion analyses, yielding lesion-function correlates based on a cytoarchitectonic model. Finally, the lesion-function correlates are validated by functional imaging reference data. *Hum Brain Mapp 30:1444–1456, 2009.* ©2008 Wiley-Liss, Inc.

Key words: tactile agnosia; texture recognition; shape recognition; lesion analysis; cytoarchitectonic probabilistic maps; double dissociation

*Correspondence to: Bruno Weder, Klinik für Neurologie, Kantonsspital St. Gallen, CH-9007 St. Gallen, Switzerland.
E-mail: bruno.weder@kssg.ch

Received for publication 15 March 2007; Revised 22 April 2008; Accepted 25 April 2008

DOI: 10.1002/hbm.20617

Published online 17 July 2008 in Wiley InterScience (www.interscience.wiley.com).

INTRODUCTION

Lesion analysis is one of the main neuroscientific tools to infer structure–function relationships. It relies on the combined analysis of a defined neurological deficit and the underlying critical brain area. Functional imaging techniques have largely superseded traditional lesion analysis

because of a number of disadvantages. Among them are the need for patients with a circumscribed brain lesion and a distinct deficit and the fact that brain function in patients is per se not healthy. Yet, suitable lesion studies of patients provide a unique window to the relationship between structure and function that is complementary to other techniques [Rorden and Karnath, 2004]. Dissociation of function is often the focus of interest, preferentially a double dissociation of function [Teuber, 1955]. In double dissociation, a lesion of structure **X** will specifically disrupt function **A** while sparing function **B**, and, conversely, a lesion of structure **Y** will specifically affect function **B** while function **A** remains intact.

In this article, we present a new hypothesis-driven method to lesion analysis, involving mapping to a stereotaxic probabilistic cytoarchitectonic atlas [Amunts and Zilles, 2001; Zilles et al., 2002]. In our approach, we make use of a unique stereotaxic probabilistic cytoarchitectonic atlas for the mapping of lesions and state of the art computational methods. The cytoarchitectonic atlas captures interindividual and interhemispheric variability of the underlying microstructurally defined cortical areas instead of macroanatomical labels of a single individual. A nonlinear, elastic registration algorithm is used to compute dense voxel-wise transformations between the brain of the patient and the reference brain of the stereotaxic atlas [Holmes et al., 1998]. The extent of the lesions is supplied to the algorithm in form of a mask. Modifications to the underlying mathematical functional ensure that the lesion is preserved in relationship to the surrounding tissue during registration [Henn et al., 2004; Henn et al., 2006]. The method is applied in a study of three patients with unilateral tactile aperceptive agnosia of one hand for everyday objects which had persisted for years after an ischemic infarction [Bohlhalter et al., 2002]. Patient 1 has a lesion in the upper part of the postcentral gyrus of the left hemisphere, Patient 3 a lesion in the superior posterior parietal lobe of the left hemisphere, and Patient 2 lesions in both regions. Hence, Patient 2 has lesions in common with both Patient 1 and 3, whereas these two have distinct lesions, allowing us to test for double dissociation. Tactile object recognition depends on the conveyance of multiple afferents from cutaneous and deep receptors in joints and muscles of an exploring hand. From the view of perception, these elementary sensations are integrated to yield more complex information reflecting the textural and spatial patterns of a specific object: Area 3a receives input primarily from muscle stretch receptors, area 3b from cutaneous mechanoreceptors. Rapidly adapting cutaneous receptors predominate in area 1. However, it also receives input converging from regions of the hand and fingers that are represented in areas 3a and 3b. Area 2 receives convergent input from slowly and rapidly adapting cutaneous receptors and proprioreceptors in the underlying muscles and joints. In parallel with the increased number of neurons with converging receptive fields along the rostrocaudal axis within the postcentral gyrus, the partitioning of the somatosensory areas becomes weaker and the complexity of the receptive fields increases [Iwamura et al., 1998]. Duffy and Burchfiel [1971] and Sakata et al. [1973] were the first to suggest a hierarchical processing of somatosensory information within the postcentral gyrus and the superior parietal lobule on the basis of single unit recordings in monkeys. They found that the receptor field neurons of Brodmann area (BA) 5 of the superior parietal lobule were larger and more complex than those of somatosensory area I (SI). O'Sullivan et al. [1994] and Roland et al. [1998] found evidence in PET activation studies of the human brain for distinct information streams depending on the somatosensory domains of microgeometry and macrogeometry. Roughness discrimination activated the lateral opercular cortex, whereas shape and length discrimination activated the anterior part of the intraparietal sulcus. In a functional magnetic resonance imaging, fMRI, study, explicit processing of shape differences between objects sequentially presented to the right hand indicated maintenance of information within the superior parietal lobule of the left hemisphere during the delay period between exploration of the first and second object. Activation of the homologue area of the right hemisphere was evoked by the final somatosensory discrimination [Stoeckel et al., 2004]. Therefore, it can be inferred that anterior parietal lesions are associated with tactile agnosia due to deficient processing of textural cues, whereas posterior lesions cause tactile agnosia, i.e., astereognosis, through deficient kinaesthetic cues.

Relying on these observations, the neurobehavioral data [Bohlhalter et al., 2002] and the aforementioned lesion locations, we predict contralateral to the affected hand an impairment of somatosensory cytoarchitectonic areas involved in the consecutive processing chain handling microscopical object properties in Patients 1 and 2. For Patients 2 and 3, we expect contraleral to the affected hand an impairment of cytoarchitectonic areas in the anterior part of the posterior parietal lobe. An impairment of these areas interferes with the processing of shape that can be predicted for patients with tactile apraxia. It involves associated shape recognition failure or distorted processing of macroscopical object properties [Binkofski et al., 2007]. Our hypothesis corresponds to the concept of dual streams of somatosensory information flow elaborated by Caselli et al. [1993], suggesting two independent functional networks serving specific information processing. From the perspective of lesion analysis, our study recovers the concept of double dissociation of function [Teuber, 1955].

To verify our hypothesis and to demonstrate the potential of the method for lesion analysis and characterization, respectively, we mapped the lesions into the stereotaxic space of the cytoarchitectonic atlas. The analysis included cytoarchitectonic areas of the postcentral gyrus (BA 3a, 3b, 1 [Geyer et al., 2000] and 2 [Grefkes et al., 2001], the neighboring precentral gyrus (BA 4a and 4p [Geyer et al., 1996]), the secondary somatosensory cortex SII of the parietal operculum including areas OP1-4 [Eickhoff et al., 2005] as

well as two areas in the anterior portion of the ventral intraparietal sulcus (IP1, IP2 [Choi et al., 2006]). Area IP1 and IP2 occupy the anterior lateral bank of the human intraparietal sulcus (IPS), IP1 being located posterior and medial to IP2. The correct human correlate of the anterior intraparietal sulcus (AIP), however, as defined in macaques is not definitely resolved. Analysing somatosensory information processing in both lesion and activation studies may contribute the resolution since the AIP is conceived as a multimodal somatosensory area serving the integration of somatosensory information [Grefkes et al., 2001; Sakata et al., 1995].

PATIENTS AND METHODS

Patients

Three patients with tactile agnosia of one hand for everyday objects that had persisted for years after an ischemic infarction were included in the study. Handedness was assessed by the Edinburgh Inventory [Oldfield, 1971]. While primary sensory perception, i.e., specifically light touch, vibration sense and position sense of forefingers, was normal, two-point discrimination was impaired in each individual.

Patient 1 was a 29-year-old, right-handed man. Cranial computed tomography (CT) revealed an arteriovenous malformation in the left parietotemporal lobe. Several embolizations of the arteriovenous malformation by endovascular techniques left neurological sequelae most likely of ischemic origin [Qureshi et al., 2000]. The clinical data were obtained following a stable course of 2 years after embolization. The MRI showed a partially embolized lesion in the left postcentral gyrus extending subcortically to the border of the lateral ventricle and ventrally to the precentral gyrus. The patient showed slight spasticity of the right upper extremity with exaggerated tendon reflexes and weakened closure of the fist. The main finding was a marked tactile agnosia of the right hand. Elementary sensations were not affected, and two-point discrimination was moderately impaired (15 mm at the tip of index finger, normal 2 mm). The results of neuropsychological testing were unremarkable. Selective attention, cognitive flexibility, and memory were also normal.

Patient 2 was a 67-year-old, right-handed woman who had suffered a left parietal ischemic infarction 30 years before the study. Persistent inability to recognize every day objects by tactile exploration with the right hand was the only clinical residuum; she had fully recovered from infarction in all other aspects. Magnetic resonance images disclosed an isolated defect within the left postcentral gyrus, extending from the Sylvian to the longitudinal fissure and involving parts of posterior parietal lobe. Neurological examination was normal except impaired two-point discrimination (55 mm at the tip of index finger), tactile apraxia, and tactile agnosia of the right hand. Neuropsychological evaluation revealed moderately impaired executive functions, while cognitive functions, notably memory, and attention were intact.

Patient 3 was a 64-year-old, right-handed man who had 4 years before the study a left posterior parietal ischemic infarction of embolic origin caused by a dissected aortal aneurysm with involvement of the supraaortal arteries. Inability to recognize everyday objects by tactile exploration with the right hand was the predominant clinical residuum. Magnetic resonance images disclosed a circumscribed defect within the left posterior parietal lobe, preferentially involving the superior parietal lobule. Additionally, circumscribed ischemic lesions involved the left medial frontal and dorsal premotor cortex and the left head of caudate nucleus. Neurological examination was normal except slightly impaired two-point discrimination (10 mm at the tip of index finger) and the tactile apraxia associated with agnosia of the right hand mentioned above. Neuropsychological evaluation revealed moderately impaired executive functions and slightly impaired verbal learning.

Prior to inclusion into the study, the subjects gave written, informed consent in accordance with the Declaration of Human Rights, Helsinki, 1975. The study is in accordance with the guidelines of the Ethics Committee of the Kantonsspital St. Gallen.

Neurobehavioral Data

The assessment of tactile object recognition and the methods for testing somatosensory discrimination in the macro- and microgeometrical domain were detailed in a previous paper [Bohlhalter et al., 2002]. A short overview is given in the following subheads.

Tactile object recognition

Primarily, tactile recognition was tested with 30 everyday objects, such as a coin, a key, or a nutshell. Objects that were not correctly identified tactually were presented again to the subjects during five specific matching tasks: (i) tactile-tactile matching with the affected hand, (ii) tactile matching of objects involving the nonaffected hand after first presentation of objects to the affected hand, and (iii) reverse, (iv) tactile-visual, and (v) visual imagination-tactile matching. In each of these tasks, the replica for 10 objects had to be identified from among five different objects.

Somatosensory discrimination in the macrogeometrical domain

Discrimination of oblongness was tested using two pairs of parallelepipeds with differences of 3.97 and 0.51 mm in the long axes, the former lying above and the latter below discrimination threshold [Weder et al., 1998]. The objects, manufactured of 95% hard aluminium, have identical volume (11.5 cm^3), mass, and surface qualities. Among object

pairs with differences from 0.44 mm to 5.01 mm in the long axis, the object pair used for the suprathreshold difference was discriminated by normal volunteers after consecutive exploration with the highest success rate (probability of a correct answer, $P = 0.95$, with 95% confidence interval, CI, 0.92–0.97). The exploration is characterized by transitive movements of the fingers, preferentially of fingers I to III, with directed motion, adapting exactly to the object.

Somatosensory discrimination in the microgeometrical domain

Using an adapted protocol from Morley et al. [1983], the patients explored, with the pad of their forefingers, synthetic surfaces with different grating profiles consisting of alternating grooves and ridges having spatial period lengths of 1,000 and 1,100 μm [Bohlhalter et al., 2002]. The average contact area of the scanning fingerpad was ≈123 mm^2 and the average contact pressure, held constant by a counterbalancing weight, was 0.6 g × wt × mm^2. Correct discrimination in normal volunteers is at $P = 0.90$ (0.88–0.92 95% CI). The exploration is characterized by intransitive, scanning movements of the index finger.

Magnetic Resonance Imaging, MRI

MRI was performed on a 1.5 Tesla MRI system (Symphony; Siemens, Erlangen). Scanning was performed in parallel to the behavioral assessment of tactile recognition years after the primary vascular lesion (see also section *Patients*). One millimeter thick contiguous slices were acquired in a sagittal plane using a T1-weighted gradient echo sequence (3D FLASH; repetition time, TR = 1960 ms; echo time, TE = 3.93 ms; flip angle, $\alpha = 15^\circ$; inversion time, TI = 1100 ms). Voxel size was 0.8 × 0.8 × 1 mm, allowing multiplanar reconstructions. Acquisition time was 8 min 23 s.

Probabilistic, Cytoarchitectonic Maps in Stereotaxic Space

Each map is based on cytoarchitectonic investigations of both hemispheres of 10 postmortem human brains (five males, five females; mean age: 64.9 years, SD = 16.9) with no history of neurological or psychiatric diseases [Amunts and Zilles, 2001; Zilles et al., 2002]. Brains were obtained from body donors in accordance with the guidelines of the Ethics Committee of the University of Düsseldorf. Handedness was unknown. MR images of the fixed postmortem brains were obtained prior to embedding and histological processing as a shape reference. Images were acquired with a T1-weighted 3D FLASH sequence covering the entire brain (flip angle = 40°, TR = 540 ms, TE = 5.5 ms). The spatial resolution was 1 × 1 × 1.17 mm. Brains were embedded in paraffin, sectioned (thickness 20 μm), and stained for cell bodies. The borders of the cortical areas were defined using an algorithmic approach based on multivariate statistics treating features of cortical profiles in every 60th section [Schleicher et al., 1999]. The histological sections were 3D reconstructed using the postmortem MR data set as a shape reference [Schormann and Zilles, 1998]. The reconstructed brain data sets were registered to the T1 weighted, single subject reference brain of the MNI [Holmes et al., 1998; Hömke, 2006]. The computed transformations were applied to the mapped cytoarchitectonic data. The probabilistic maps were created by superposition of the mapped areas for all ten brains. The whole method has been detailed by Amunts et al. [2000].

Definition of the Lesion Volume

The lesions in the magnetic resonance images were manually segmented by an expert (F.B.). Views of all three sectioning planes and volume renderings where used during segmentation. The result was a volume data set of identical size as the patient data set, indicating whether a voxel belongs to a lesion or not.

Registration With Incomplete Information

Registration is the process of transforming a data set such that it becomes "similar" to another data set. A number of different terms are used for that process in the literature, e.g., warping, normalization, alignment, matching. We register one data set **T**, the so-called template, to another data set **R**, the so-called reference, by minimizing the functional $\int_\Omega \mathbf{D}[T, R, \Omega; \Phi] + \alpha \mathbf{R}[\Omega; \Phi]$ on the image domain Ω. The result is a nonlinear transformation $\Phi : x \mapsto x - u(x)$ which is a translation in each point. **D** measures the distance between the reference data set and the transformed template data set $T \circ \Phi$. The regularization term **R** restricts the class of permissible transformations by penalizing transformations that are not concurrent with the model. Here, we use the sum of squared differences (SSD) of the gray values as the distance measure **D**. The regularization term **R** is the potential of the elastic energy of the transformation. The positive real scalar parameter α determines the influence of the regularization term. Applying the calculus of variation to the minimization problem yields an iterative procedure where a large system of partial differential equations (PDE) has to be solved in each step. The system of PDEs is solved with a multigrid solver. A multiresolution framework is wrapped around the iteration to facilitate efficiency and robustness of the algorithm [Henn et al., 2004; Henn et al., 2006; Hömke, 2006].

In the case of lesions, the distance measure has to be augmented to compensate for the structural distortion introduced by the lesion, e.g., large regions of atypical pixel intensity values. Minimization of the distance in that region does not reflect the objective goal of registration, i.e., the lesion is not preserved within the context of the surrounding data. Consider for example a white matter lesion with low gray values surrounded by white matter

with high gray values. Pulling the surrounding tissue inside the lesion, even contracting the lesion to zero volume, would minimize the distance between the data sets in that case.

To preserve the lesion during registration we adopted techniques from the well studied field of variational "image inpainting" [Bertalmio et al., 2000; Chan and Shen, 2002]. Hereby, missing or damaged fields, or parts of the image, are marked and supplied to the inpainting algorithm. These parts of the image are also reconstructed by minimizing a functional that consists of a distance term and a regularization term. The functional is designed such that the resulting equations in the marked regions are governed only by the regularization term, which determines how the surrounding image information is continued into the marked regions.

Applying the same techniques in this context leads to the modified distance measure $\mathbf{D}_\epsilon[T, R, \Omega, G; \Phi]$ where G is the marked region and $\mathbf{D}_\epsilon[T, R, \Omega, G; \Phi] = 0$ for all $x \in G \circ \Phi$. The regularization term $\mathbf{R}$ then "interpolates" the transformation into the region G, moving the region along with the rest of the image. In our application, the lesion region G is determined by an expert and is supplied to the algorithm as a voxel mask. The computed transformation is applied to the mask of the lesion. The transformed lesion can then be compared to the cytoarchitectonic data included in the atlas. For verification, the method has been applied to artificially lesioned data sets, facilitating the comparison with the results for the complete data sets. Similar sized lesions, in the vinicity of the lesions under investigation here, were used in these tests [Henn et al., 2006]. A similar cost-function masking technique has also been proposed by Brett et al. [2001] for the SPM normalization algorithm. This article also contains a number of tests that underline the necessity and validity of the approach in case of incomplete image information. It has been used in a number of SPM-guided studies to exclude lesions or artefacts, e.g., signal dropout.

Mapping of the Lesion Into the Space of the Cytoarchitectonic Maps

The patient data sets were compared with the stereotaxic probabilistic cytoarchtectonic atlas. Linear transformations between the patient data sets and the reference brain were computed to compensate for gross differences in overall size, orientation, and shape. Information about the lesion was not included in the computation since the local distortion has no significant impact on the global transformation. Depending on the size of the lesion, the technique described above must be applied to the cost function of the linear registration to obtain reasonable results. In the next step, the nonlinear registration method described above was applied to the linearly registered data sets. The lesions are transformed to the stereotaxic reference space by application to the lesions masks of the same linear and nonlinear transformations. 50% maps, comprising the volumes delimited by the 50% isocontours (the regions where for at least five brains of a cytoarchitectonic area overlays after registration the reference space), were calculated for the coregistration of lesion masks and cytoarchitectonic maps. The following nine cytoarchitectonic areas were compared with the lesion masks: BA 3a, 3b, and BA 1 [Geyer et al., 2000], BA 2 [Grefkes et al., 2001], BA 4a and 4p [Geyer et al., 1996], areas IP1 and IP2 [Choi et al., 2006], and areas OP1-4 [Eickhoff et al., 2005]. The number of coinciding voxels located in the cytoarchitectonic maps and the lesion, providing information about which cytoarchitectonic areas are likely to be affected and to which extent they might be affected by the lesion, was calculated.

Functional Imaging Reference Data

In a previous study, we explored somatosensory discrimination in the macroscopical domain using event-related functional imaging in seven healthy subjects [Stoeckel et al., 2004]. The activation paradigm and the parameters tested were exactly the same in this study as mentioned above in the respective section. We found one area in the left superior parietal cortex related to the maintenance of tactile object information during the delay period beween exploration of the first and second object, i.e., activation related to distinguishable objects with suprathreshold differences of 3.97 in the long axis (contrasted with the activation related to object pairs below the discrimination threshold). This area, representing explicit perception of the intended information, is introduced into the cytoarchitectonically mapped lesion of the reference brain.

RESULTS

Tactile Object Recognition

In summary, tactile recognition of 30 everyday objects, such as a coin, a key, or a nutshell, was reduced in all three patients. While Patients 2 and 3 recognized only one out of 30 objects by tactile exploration with the affected right hand, performing the task at the level of pure guessing, Patient 1 was able to recognize 9 out of 30 objects correctly. The results were stable during an observation period of one year. Tactile–tactile matching with the affected hand resulted in an enhanced, but only implicit identification of object replicas. "Crossed" tactile–tactile matching, i.e., tactile matching of objects involving the nonaffected hand after presentation of objects first to the affected hand and reverse, yielded a considerably enhanced object recognition rate in both patients. Tactile-visual and visual imagination-tactile matching using supramodal pathways resulted in equally enhanced recognition of objects in both patients. Tactile agnosia was therefore assessed as unilateral and aperceptive in nature, since association had been shown to function as evidenced by the matching tasks (Table I).

TABLE I. Neurobehavioral data

	Patient 1	Patient 2	Patient 3
Tactile object recognition[a]			
A. Affected right hand	0.3 (0.15–0.50)	0.03 (0–0.10)	0.03 (0–0.10)
B. Normal left hand	1	1	0.97 (0.83–1)
Somatosensory discrimination[b]			
A. Macrogeometric domain			
Length difference in the major axis of cuboids (Δl = 3.97mm)[c]			
Right hand	0.9 (0.77–0.96)	0.7 (0.57–0.8)[d]	0.48 (0.33–0.63)[d]
Left hand	0.98 (0.87–1)	1 (0.91–1)	1 (0.91–1)
B. Microgeometric domain			
Difference in grating profile (10% from a reference spatial period of 1000 μm)[e]			
Right hand	0.65 (0.52–0.76)[d]	0.68 (0.56–0.79)[d]	0.83 (0.7–0.91)
Left hand	0.97 (0.88–0.99)	0.87 (0.76–0.93)	1 (0.91–1)

[a] Probability of a correct answer according to proportion, incl. 95% confidence interval (Clopper-Pearson).
[b] Probability of a correct answer according to a logistic model, incl. 95% confidence interval. Because of the dichotomous approach 0.5 represents an answer by chance and 1 100 % correct responses.
[c] Normals 0.95 (0.93–0.96).
[d] SSD task performance significantly reduced compared with normal volunteers by $P < 0.001$ (one sample analysis, two tailed).
[e] Normals 0.90 (0.87–0.92).

Somatosensory Discrimination in the Macrogeometrical Domain

In Patients 2 and 3, somatosensory discrimination of the object pairs, i.e., parallelepipeds with a suprathreshold difference in the long axis, was significantly reduced in the affected hand ($P < 0.001$). Discrimination of the same objects in Patient 1 was practically preserved in the affected hand, as reflected in a score in the lower range of normal volunteers. Task performance with the nonaffected left hand was normal in all patients. Notably, tactual exploration involving the critical transitive movements of the affected right hand was severely impaired in Patients 2 and 3, who showed a slowed and irregular pattern adapted insufficiently to the objects explored (see somatosensory discrimination in Table I).

Somatosensory Discrimination in the Microgeometrical Domain

On the affected right side, the somatosensory discrimination of roughness, as represented by different grating profiles, was significantly reduced in Patients 1 and 2 compared with normal volunteers ($P < 0.001$). In Patient 3, somatosensory discrimination of roughness was slightly but insignificantly reduced. With the left hand, the probability of correct answers was in the range of normal volunteers in all patients (see somatosensory discrimination in Table I).

Comparison of Task Performances in the Macrogeometrical and Microgeometrical Domain

Task performances of Patients 1 and 3, evidencing disjoint lesions in the lesion analysis (see below), were directly compared by calculating their odds ratio (OR) from the results of Table I (somatosensory discrimination). The result, OR = 9.95 with 95% CI: 2.97–33.31, indicates that macrogeometrical somatosensory discrimination was significantly better in Patient 1 than in Patient 3. In contrast, microgeometrical somatosensory discrimination was significantly worse in Patient 1 than in Patient 3 as indicated by the OR = 0.37 with 95% CI: 0.15–0.94. As expected, both domains of task performance in Patient 2, whose lesion covered both critical subfields, i.e., in the postcentral gyrus and the posterior parietal lobe (see below), was significantly diminished.

Mapping the Lesions to the Cytoarchitectonic Atlas

In Patient 1, the lesion includes the postcentral gyrus and the anterior part of the motor areas. In Patient 2, the lesions include the postcentral gyrus and the posterior parietal cortex. Patient 3 has a lesion in the posterior parietal cortex, and additional circumscribed lesions in the left fronto-mesial and dorsal premotor cortex and the head of caudate nucleus. Figure 1A,C,E show volume renderings of the patients' brains with the lesions before non-linear registration to the atlas brain. Corresponding volume renderings after non-linear registration are displayed in Figure 1B,D,F. Both renderings of the patients' brains match the atlas brain while the lesions are preserved within the context of the surrounding tissue. Table II summarizes the overlap between the 50%-probabilistic maps and the transformed lesion masks.

Concerning the lesion in the postcentral gyrus in Patient 2, the main overlap is found in BA 1 and 2. In Patient 1 mainly BA 3a and 3b are involved. As Table II shows, the lesions of Patient 1 and 2 coincide in BA 1,2, and 3b. These areas cover over 90% of the coinciding lesion and each contributes about 30% to that overlap. The parietal opercu-

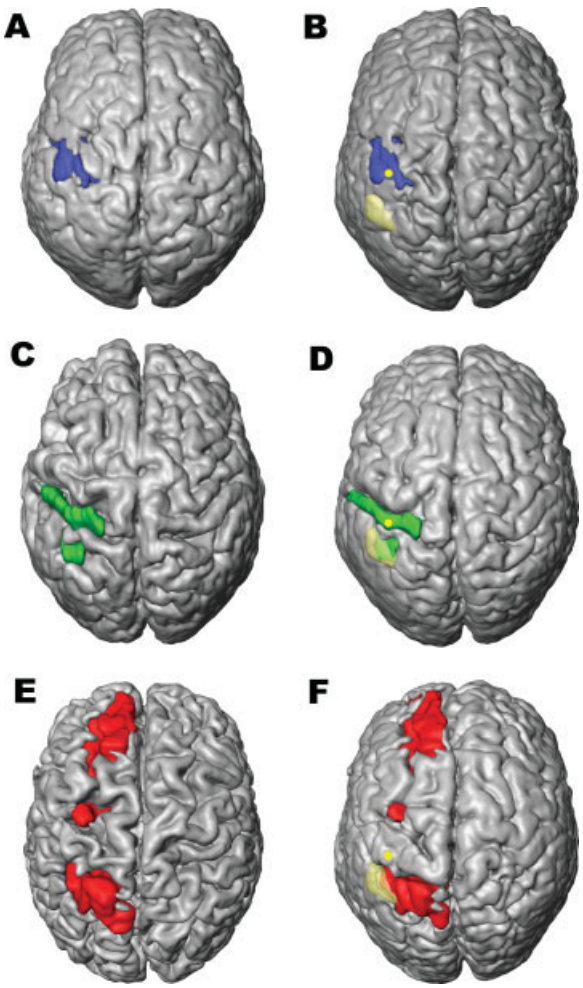

Figure 1.

Surface renderings of the patients brain before and after nonlinear registration to the reference brain. The reference brain of the atlas is the single subject template of the MNI [Holmes et al., 1998]. Patient 1–3 are shown from top to bottom (**A**,**C**,**E** = original brains, **B**,**D**,**F** = after nonlinear transformation to reference space). In Patient 1 the lesion includes the postcentral gyrus and the anterior part of the motor areas. In Patient 2 the lesions include the postcentral gyrus and the posterior parietal cortex. Patient 3 has a lesion in the posterior parietal cortex, and additional lesions in the left medial frontal cortex and—very circumscribed—in the left dorsal premotor cortex. The transparent yellow area in B,D,F marks the projection of the activation field described in the study of Stoeckel et al. [2004], i.e., activation during maintenance of kinaesthetic information on line (MNI space coordinates of the center of gravity $x = -48$, $y = -50$, $z = 54$). The yellow dot represents the centre of gravity of the hand area in the postcentral gyrus, projected onto the cortical surface, found by Boecker et al. [1995] in a somatosensory activation task. Note: The study of Stoeckel et al. [2004] employed the same task for perception within the macrogeometrical domain as the present study. Both studies are based on the identical cytoarchitectonic maps of areas IP1 and IP2.

lum, i. e. areas OP1-4 [Eickhoff et al., 2005], were not affected by any of the lesions. The patients' lesions do not involve the whole somatosensory cortex, but mainly the somatosensory hand areas centered at $x = -40 \pm 6$ (SD), $y = -39 \pm 5$ (SD) and $z = 50 \pm 4$ (SD) in the space of Talairach and Tournoux [1988]. At these coordinates activation was demonstrated in a somatosensory activation task of the right hand in a group of healthy subjects [Boecker et al., 1995]. In addition, the hand area of the motor cortex and, thus, the neighbouring somatosensory cortex, can be estimated by a knob on the precentral gyrus [Yousry et al., 1997]. Slices for Figures 2–4 were selected on the basis of these criteria. The involvement of the cytoarchitectonic areas in these slices is illustrated for Patient 1 in Figure 2, for Patient 2 in Figure 3, and for Patient 3 in Figure 4. The lesion is shown as a white contour, and the cytoarchitectonic areas are color coded: dark green = BA 4a, light green = BA 4p, red = BA 3a, orange = BA 3b, yellow = BA 1, blue = BA 2, purple = area IP1, magenta = area IP2.

The lesions in the posterior parietal lobe of Patient 2 and 3 were not fully characterized with respect to their cytoarchitectonic correlates. This region has not yet been described cytoarchitectonically with the exception of two cytoarchitectonic areas of the intraparietal sulcus, IP1 and IP2 [Choi et al., 2006]. However, both patients share a lesion pattern involving both parts of the intraparietal sulcus and the superior parietal lobule.

The ventral intraparietal area IP1 (purple) overlaps with the posterior lesions in Patient 2 and 3 (see Table II, Figs. 3 and 4). Note that the portion of IP1 covered by the lesions is almost identical in Patients 2 and 3. In Patient 2 the lesion overlaps slightly with IP2 (magenta) (see Table II and Fig. 3). Only a few voxels of IP2 covered by the lesion of Patient 2 coincide with the lesion of Patient 3. In a recent study employing the same task in the macrogeometrical domain as in this study, we found evidence for the activation of areas IP1 and IP2 during maintenance of tactile object information in healthy volunteers [Stoeckel et al., 2004]. In other words, this area in the left hemisphere indicated the activation related to keeping explicitly perceived kinaesthetic information in memory. The border of the observed activation is marked in the surface rendering of the reference brain in Figure 1B,D,F. The area includes the superior parietal lobule and the adjacent intraparietal sulcus, preferentially its dorsal part. Furthermore, it should be noted that the corresponding behavioral data for somatosensory discrimination in the macroscopical domain obtained in the study by Stoeckel et al. [2004] are integrated as reference data in Table I.

The comparison of functional imaging reference and lesion data suggests a dichotomy of tactile recognition into subfunctions: The activation field obtained after somatosensory discrimination in the macroscopical domain fits perfectly with the lesion in the posterior parietal lobe of those patients exhibiting dysfunctional shape recognition. In contrast, the lesion common to those patients with

TABLE II. Involvement of cytoarchitectonic areas as measured by the 50% isocontour

Anatomical structure	Cytoarchitectonic area	Patient 1 Lesion extent [%]	Patient 2 Lesion extent [%]	Patient 3 Lesion extent [%]	Patient 1&2 Lesion extent [%]	Patient 2&3 Lesion extent [%]
Precentral gyrus	4a	24.4	0	0	0	0
Precentral gyrus	4p	69.5	0	0	0	0
Postcentral gyrus	3a	67.5	0	0	0	0
Postcentral gyrus	3b	50.6	10.7	0	5.4	0
Postcentral gyrus	1	18.5	32.9	0	6.9	0
Postcentral gyrus	2	25.2	31.1	0.4	7.7	0
Intraparietal sulcus	IP1	0	44.7	78.7	0	42.2
Intraparietal sulcus	IP2	0	1.2	0	0	0
Parietal operculum	OP1-4	0	0	0	0	0

dysfunctional texture recognition is far outside of this activation field and projects to the hand area in the postcentral gyrus. It should be noted that the use of functional imaging reference data may be preferable to anatomical reference data since they do not include effects of local reorganization which have been observed after stroke [Jaillard et al., 2005].

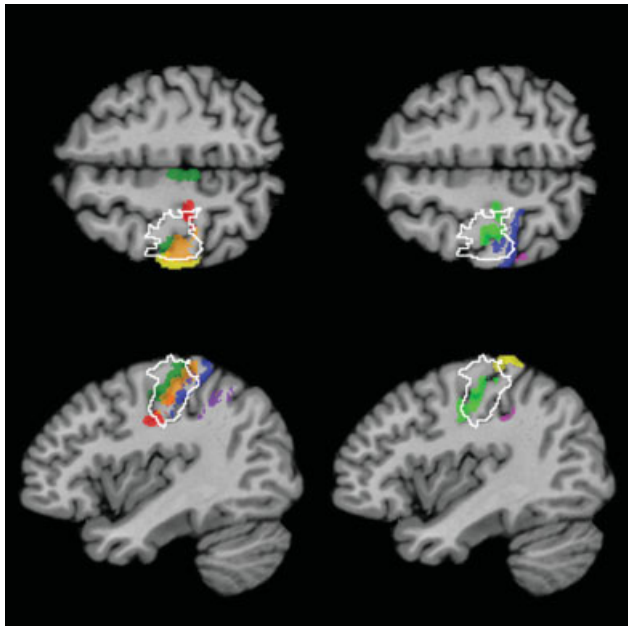

Figure 2.
Overlap of the 50% isocontour of the cytoarchitectonic areas with the lesion (white contour line) in common reference space for Patient 1. Horizontal and sagittal sections through the hand area as defined by the average z- and x-coordinates of Boecker et al. [1995]. The lesion overlaps with areas BA 3a and 3b of the anterior bank of the postcentral gyrus and BA 4a and 4p of the motor cortex. *Color coding*: dark green = BA 4a, light green = BA 4p, red = BA 3a, orange = BA 3b, yellow = BA 1, blue = BA 2, purple = area IP1, magenta = area IP2.

DISCUSSION

The proposed method for lesion quantification provides a new and important way to study the relationship between lesions and function. On the basis of the quantification of subfunctions underlying tactile recognition, we predicted in three patients the involvement of the critical neural structures involved, substantiating proposals found in the literature. The implication of the expected areas and their assignment to microstructurally defined cortical areas substantiates our approach.

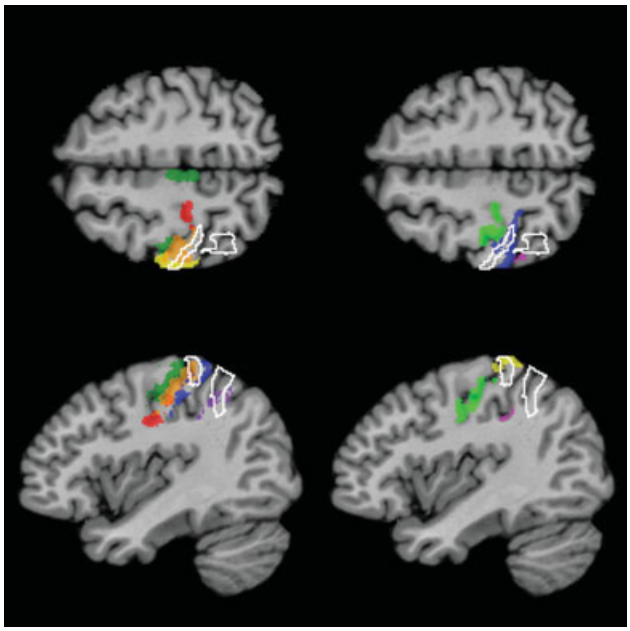

Figure 3.
Same as Figure 2, but for Patient 2. The overlap of the lesion and the cytoarcitectonic areas shows the involvement of the posterior bank of postcentral gyrus, mainly BA 1 and BA 2, and areas IP1 and IP2 in the intraparietal sulcus. The lesion involves the adjacent superior parietal lobule. *Color coding*: dark green = BA 4a, light green = BA 4p, red = BA 3a, orange = BA 3b, yellow = BA 1, blue = BA 2, purple = area IP1, magenta = area IP2.

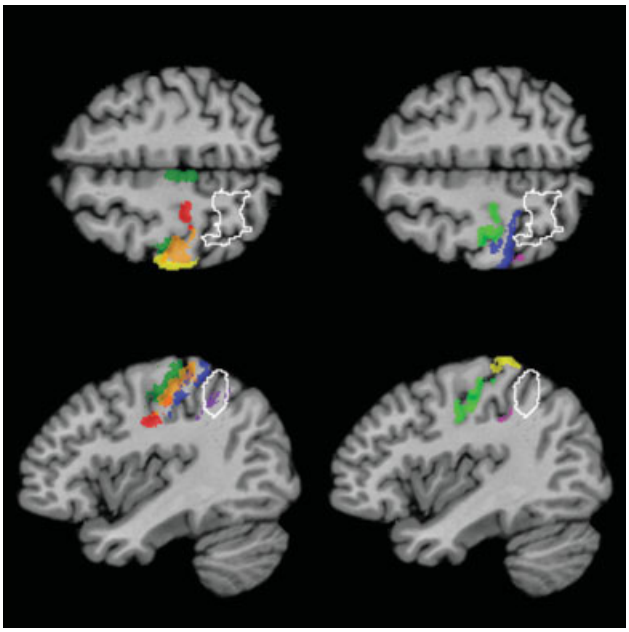

Figure 4.
Same as Figure 1, but for Patient 3. The lesion overlaps preferentially with area IP1 in the intraparietal sulcus and involves the adjacent superior parietal lobule. *Color coding*: dark green = BA 4a, light green = BA 4p, red = BA 3a, orange = BA 3b, yellow = BA 1, blue = BA 2, purple = area IP1, magenta = area IP2.

All three patients exhibited features of unilateral tactile aperceptive agnosia; to varying degrees, they had difficulties to recognize everyday objects. This deficit could be attributed to a dysfunction of one hemisphere. In Patient 1, perception of microgeometrical object properties characterizing their surfaces (i.e., grating profiles) was impaired, in Patient 3, the perception of macrogeometrical object properties associated with their shape (i.e., the oblongness of cuboids) [Johnson and Hsiao, 1992; Roland and Mortensen, 1987; Sathian, 1989], whereas patient 2 showed both deficits. As inferred from impaired textural recognition, the disintegration of the functional chain of consecutive cytoarchitectonic areas within the postcentral gyrus, which constitutes part of a distinct functional system for texture information processing, was verified in Patients 1 and 2. Additionally, as deduced from impaired kinaesthetic information processing, the critical involvement of the superior parietal lobule and the intraparietal sulcus, constituent part of a second functional system, was verified in Patients 2 and 3. Thus, the disparate disruption of cytoarchitectonic areas in Patients 1 and 3 corresponds to the loss or preservation, respectively, of subfunctions underlying tactile agnosia, an example of double dissociation [Teuber, 1955]. This relation between the affected cytoarchitectonic areas, including the neighbouring superior parietal lobule, is further substantiated by the findings pertaining to Patient 2, which showed lesions and dysfunctions in common with Patients 1 and 3.

Since discrimination paradigms probing the micro- and macrogeometrical domains are not associated with real perceptions of specific objects, the dysfunction in our patients that impeded explicit recognition of objects would be unimodally caused by impaired processing of elementary sensory cues. Furthermore, the patients were able to transfer sensory information to and from the contralateral intact hemisphere and the visual association cortices.

Thus, they obviously had access to unimodal or polymodal association fields and were able to compensate explicitly for the inappropriate percept acquired by the affected hand (see matching tasks). There were no indications of conceptual deficits implying associative tactile agnosia [Caselli, 1993; Mesulam, 1998; Reed et al., 1996]. Finally, the patients with the impaired perception in the macroscopical domain showed disrupted transitive movements characteristic of tactile apraxia [Binkofski et al., 2001].

On the basis of these observations, we conjectured in the patients with impaired texture recognition degradation of sequential processing within the somatosensory areas located in the postcentral gyrus ascribed to Brodmann areas (BA) 3a, 3b, 1, 2. In the patients with impaired shape recognition, we conjectured disrupted parallel processing in the superior parietal lobule and the adjacent intraparietal sulcus, the latter being more implicated in the cytoarchitectonic area IP1.

After lesion of cytoarchitectonic areas within the postcentral gyrus as in Patients 1 and 2, elementary responses in 3a and 3b from single deep and cutaneous receptor fields cannot be integrated with cues encoding movement direction of single digits, nor finally converted into multidigit cues in BA 1 and 2 [Iwamura, 1998]. The inferred disintegration of information processing in the rostrocaudal direction is reflected primarily by the attenuated two-point discrimination, a relatively simple result deduced from the serial processing of elementary sensations [Johnson and Phillips, 1981]. In the feed-forward direction, the cortex lining the intraparietal sulcus and the anterior part of the supramarginal gyrus are presumed to belong to this chain of hierarchical information processing of somatosensory representations [Bodegard et al., 2001]. From the behavioral data obtained in the matching tasks, we can conclude that the interference between somatosensory and visual information, conjectured to take place in superior parietal area BA 5, may have been spared in our patients [Iwamura, 1998]. In addition, the overlap of the lesion of Patient 1 with the motor areas BA 4a and 4p did not result in observable deficits.

The areas of the superior parietal lobule and parts of intraparietal sulcus are, together with the ventral premotor cortex, constituents of a fronto-parietal circuit for object manipulation, as evidenced, e.g., in a fMRI study by Binkofski et al. [1999]. Accordingly, patients with posterior parietal lobe lesions exhibit a distinct unimodal apractic disorder, i.e., tactile apraxia, characterized by disrupted

transitive movements as observed in Patients 2 and 3 [Binkofski et al., 2001]. Recently, we showed that the region lesioned in these patients was active when healthy volunteers perceived explicit somatosensory cues [Stoeckel et al., 2004]. We applied the same cytoarchitectonic maps for structure-functional comparison, and as in our lesion study, the activated region was identified in the superior parietal lobule, the ventral intraparietal (IP1) and the anterior intraparietal sulcus (IP2) [Choi et al., 2006]. Recently, the horizontal segment of the intraparietal sulcus has been shown to mediate changes in stimulus configuration [Molenberghs et al., 2007]. Hence, AIP seems to constitute one of the most important interfaces between action and perception in the haptic system [Binkofski et al., 2007]. The definition of its human homologue within IP1 or IP2 is a compelling future activity related to lesion and activation studies exploring somatosensory information processing. In conclusion, we conjecture that processing of shape or kinaesthetic information, respectively, was disrupted in these subjects. There remains the question of interference between the additional ischemic lesions and task performance in Patient 3. A crucial observation is that the ventral premotor and opercular, ventral and anterior prefrontal cortices, important relay nodes for manipulation and working memory processes during the task [Binkofski et al., 1999; Stoeckel et al., 2003], were preserved. Thus, and most important, the distinctive impairment of the subfunction for kinaesthetic information processing described above is clearly related to the specific processor in the posterior parietal lobe.

The hypothesis-driven strategy employed here shows some important differences to the exploratory strategies generally used in lesion studies. Exploratory strategies seek to identify a structure-functional relationship by trying to find a common denominator of a large sample of patients with brain lesions and the same behavioral deficit. Generally, the patients have various deficits and their lesions may affect a number of areas. To enhance the discrimination power, control groups of patients without the deficit in question, yet with lesions in similar areas of the brain, i.e., large samples of reference brains, can be used [Karnath et al., 2004; Rorden and Karnath, 2004]. The resulting statistical parametric maps indicate the part of the lesion most likely associated with the behavioral deficit. In contrast, we follow an alternative proposal of the international consortium for Brain Mapping, which explicitely proposed the collection of small samples of target brains subject to detailed cytoarchitectural and chemoarchitectural analyses to form a very information-rich ultimate dataset [Mazziotta et al., 2001]. We start from a working hypothesis and compare the lesions to an atlas, namely the cytoarchitecture derived from a sample of postmortem brains. That enables us to investigate the lesions with respect to not only what they have in common, but to the subtle differences between individual lesions. The findings confirm that different neural processes may subserve somatosensory perception- and action-related information processing. These two separate routes of tactile processing have been elaborated recently by Dijkerman and de Haan [2007], one projecting through the SII to the insula and another terminating in the posterior parietal areas. Our data substantiate this hypothesis of segregated paths for perception-related information processing in SI and the connected SII and action-related information processing in the posterior parietal lobe. This assumption is confirmed by the transformation of our functional imaging reference data of healthy subjects into the common stereotaxic space of the reference brain [Rorden and Karnath, 2004]: (i) the activation field reflecting perception of kinaesthetic information projects exactly onto the lesion in the superior parietal lobule and the adjacent intraparietal sulcus of the patients with impaired shape recognition [Stoeckel et al., 2004] whereas (ii) the lesion common to those individuals with impaired texture recognition projects onto the hand area of the postcentral gyrus determined by the coordinates reported by Boecker et al. [1995] in a somatosensory activation task. The partition into parallel sensory information processing is supported by the anatomic paths traced in monkeys, in which most somatosensory information from the thalamus enters the cerebral cortex through projections from the ventrobasal complex to SI, but small projections exist also between the anterior nucleus of the pulvinar and the lateral posterior nucleus to BA 5 [Jones et al., 1979].

An important component of any lesion analysis is compensation for interindividual variability, i.e., the transformation of different brains and their lesions into a common reference space. The accuracy of the findings depends directly on the extent to which differences in the size and shape of the brains are compensated. Interactive techniques have frequently been used to transfer lesions into a common reference space. Fiez et al. [2000] used manual techniques implemented in the BrainVox software package, relying on the "eyeball norm" to fit coronal slices. Caviness et al. [2002] transformed their data sets to Talaraich space [Talairach and Tournoux, 1988], and parcellated the lesion based on corresponding structures in the unaffected hemisphere. Karnath et al. [2004; 2001] manually drew the lesions on visually corresponding slices of the reference brain using every eighth slice in the region of interest. A major disadvantage of manual methods, however, is the application of observer-dependent concepts in defining the correspondence of healthy and injured structures. These methods, therefore, include a strong subjective component.

Automatic alignment of brain data sets does not suffer from this disadvantage. Yet, when the lesion is automatically mapped into the reference space, the type of the transformation plays a crucial role. Simple global linear transformations account for differences in size, rotation, and translation. The position of macroscopical features of the brain such as sulci and gyri, however, can vary on the order of centimeters among individuals. To accommodate such differences, local nonlinear transformations are

needed. Moreover, the presence of lesions necessitates extension of standard methods to deal with the structural distortion introduced by the lesion. Mort et al. [2003] used a modification of the non-linear registration technique of SPM (Statistical Parametric Mapping http://www.fil.ion.ucl.ac.uk/spm/) toolbox [Brett et al., 2001], as did Karnath et al. [2005] in a recent study. The method is quite similar to our registration algorithm, but differs in two respects: First, the modeling of the registration problem is different, i.e., the constraints on the solution differ. Second, and more importantly, our method computes a dense transformation at the resolution of the data set, i.e., a displacement vector for each voxel implying $256 \times 256 \times 256 \times 3$ unknowns, whereas SPM, as applied by Karnath et al. [2005] and Mort et al. [2004], only computes transformations with $8 \times 8 \times 9$ coefficients. High spatial resolution is a necessary prerequisite for the analysis of individual data sets. The spatial resolution of the effect to be studied depends on the spatial resolution of the transformation. Although high spatial resolution of the transformation would increase the discrimination power in group studies, it plays a less important role there, since a common denominator, not the evaluation of individual differences, is sought. Lesion mapping using automated image registration has several limitations: (i) the computed transformation between the space of the subject's brain and that of the reference brain depends on structural correspondence between both brains. Since a lesioned brain region, however, contains no information about the structure of the brain, or it contains distorted information, structural correspondence cannot be established for these regions. As a consequence, the transformation must rely on information from the transformation of the surrounding areas. When lesions are manually transferred, the putative borders between lesioned and non-lesioned tissue in the reference brain constitute the new lesion contour. When automatic registration algorithms with cost-function masking are used, information about the transformation in the surrounding area is continued into the region of the lesion using smoothness constraints on the transformation. The accuracy of the spatial localization within the lesion thus decreases with the distance from its border, implying that transformation of very large lesions cannot be performed with high accuracy. In the present study, the lesions are small and circumscribed, enabling an accurate comparison with the cytoarchitectonic maps.

CONCLUSIONS

The superposition of brain lesions of three patients with aperceptive tactile agnosia on cytoarchitectonic maps supports the hypothesis of the differential impairment of two independent functional systems subserving somatosensory discrimination in the microscopical and macroscopical domain. Normal function of these systems is the precondition for the perception of surface characteristics and the shape of objects. Circumscribed lesions that interfered with these functions, were delineated as voxel masks, and the individual brains and voxel masks were transformed into the space of a common reference brain. Using a stereotaxic cytoarchitectonic probabilistic atlas, the involvement of the lesion was quantified with respect to cortical areas of the postcentral gyrus and the intraparietal sulcus. The lesion-function correlates are validated finally by the transformation of functional imaging reference data of healthy subjects into the common stereotaxic space of the reference brain. This opens the perspective of modeling lesions causing specific dysfunctions based on microstructurally defined cortical areas.

ACKNOWLEDGMENTS

We thank Dr. John Missimer from PSI Villigen for careful reading of the manuscript and suggestions and Professor Alex Keel from the Institute for Statistics and Mathematics of the University of St. Gallen for the help in statistical analysis of the data.

REFERENCES

Amunts K, Zilles K (2001): Advances in cytoarchitectonic mapping of the human cerebral cortex. In: Naidich TP, Yousry TA, Mathews VP, editors. Anatomic Basis of Functional MR Imaging, 11 ed. Philadelphia: Harcourt. pp 151–169.

Amunts K, Malikovic A, Mohlberg H, Schormann T, Zilles K (2000): Brodmann's Areas 17 and 18 brought into Stereotaxic Space—Where and How Variable? Neuroimage 11:66–84.

Bertalmio M, Sapiro G, Caselles V, Ballester C (2000): Image inpainting. In: Akeley K, editor. Siggraph 2000, Computer Graphics Proceedings. Munich: ACM Press/ACM SIGGRAPH/Addison Wesley Longman. pp 417–424.

Binkofski F, Buccino G, Posse S, Seitz RJ, Rizzolatti G, Freund H (1999): A fronto-parietal circuit for object manipulation in man: Evidence from an fMRI-study. Eur J Neurosci 11:3276–3286.

Binkofski F, Kunesch E, Classen J, Seitz RJ, Freund HJ (2001): Tactile apraxia: Unimodal apractic disorder of tactile object exploration associated with parietal lobe lesions. Brain 124:132–144.

Binkofski F, Reetz K, Blangero A (2007): Tactile agnosia and tactile apraxia: Crosstalk between the action and perception streams in the anterior intraparietal area. Behav Brain Sci 30:2001–2002.

Bodegard A, Geyer S, Grefkes C, Zilles K, Roland PE (2001): Hierarchical processing of tactile shape in the human brain. Neuron 31:317–328.

Boecker H, Khorram-Sefat D, Kleinschmidt A, Merboldt K-D, Hänicke W, Requart M, Frahm J (1995): High-resolution functional magnetic resonance imaging of cortical activation during tactile exploration. Hum Brain Mapp 3:236–244.

Bohlhalter S, Fretz C, Weder B (2002): Hierarchical versus parallel processing in tactile object recognition: A behavioural-neuroanatomical study of aperceptive tactile agnosia. Brain 125:2537–2548.

Brett M, Leff AP, Rorden C, Ashburner J (2001): Spatial normalization of brain images with focal lesions using cost function masking. Neuroimage 14:486–500.

Caselli RJ (1993): Ventrolateral and dorsomedial somatosensory association cortex damage produces distinct somesthetic syndromes in humans. Neurology 43:762–771.

Caviness VS, Makris N, Montinaro E, Sahin NT, Bates JF, Schwamm L, Caplan D, Kennedy DN (2002): Anatomy of stroke, Part I: An MRI-based topographic and volumetric system of analysis. Stroke 33:2549–2556.

Chan TF, Shen J. (2002): Mathematical models for local nontexture inpaintings. SIAM J Appl Math 62:1019–1043.

Choi HJ, Zilles K, Mohlberg H, Schleicher A, Fink G, Amstrong E, Amunts K (2006): Cytoarchitectonic identification and probabilistic mapping of two distinct areas within the anterior ventral bank of the human intraparietal sulcus. J Comp Neurol 495:53–69.

Dijkerman H, de Haan E (2007): Somatosensory processes subserving perception and action. Behav Brain Sci 30:189–239.

Duffy FH, Burchfiel JL (1971): Somatosensory system: Organizational hierarchy from single units in monkey area 5. Science 172:273–275.

Eickhoff SB, Amunts K, Mohlberg H, Zilles K (2005): The human parietal operculum. II. Stereotaxic maps and correlation with functional imaging results. Cerebral Cortex 16:268–279.

Fiez JA, Damasio H, Grabowski TJ (2000): Lesion segmentation and manual warping to a reference brain: Intra- and interobserver reliability. Hum Brain Mapp 9:192–211.

Geyer S, Ledberg A, Schleicher A, Kinomura S, Schormann T, Burgel U, Klingberg T, Larsson J, Zilles K, Roland PE (1996): Two different areas within the primary motor cortex of man. Nature 382:805–807.

Geyer S, Schormann T, Mohlberg H, Zilles K (2000): Areas 3a, 3b and 1 of human primary somatosensory cortex: II. Spatial normalization to standard anatomical space. Neuroimage 11:617–632.

Grefkes C, Geyer S, Schormann T, Roland P, Zilles K (2001): Human somatosensory area 2: Observer-independent cytoarchitectonic mapping, interindividual variability, and population map. Neuroimage 14:617–631.

Henn S, Hömke L, Witsch K (2004): Lesion Preserving Image Registration with Applications to Human Brains. Pattern Recognition: 26th DAGM Symposium, Tuebingen, Germany, August 30–September 1, 2004. Proceedings, 3175 ed. Wien, New York: Springer. pp 496–503.

Henn S, Hömke L, Witsch K (2006): A generalized image registration framework using incomplete image information—With applications to lesion mapping. In Scherzer O, editor. Mathematical Models for Registration and Applications to Medical Imaging. Wien, New York: Springer. pp 3–26.

Holmes CJ, Hoge R, Collins L, Woods R, Toga AW, Evans AC (1998): Enhancement of MR images using registration for signal averaging. J Comp.Assisted Tomogr 22:324–344.

Hömke L (2006): A multigrid method for anisotropic PDEs in Elastic Image registration. Num Linear Algebra Appl 13:215–229.

Iwamura Y (1998): Hierarchical somatosensory processing. Curr Opin Neurobiol 8:522–528.

Jaillard A, Martin CD, Garambois K, Lebas JF, Hommel M (2005): Vicarious function within the human primary motor cortex? A longitudinal fMRI stroke study. Brain 128:1122–1138.

Johnson KO, Hsiao SS (1992): Neural mechanisms of tactual form and texture perception. Annu Rev Neurosci 15:227–250.

Johnson KO, Phillips JR (1981): Tactile spatial resolution. I. Two-point discrimination, gap detection, grating resolution, and letter recognition. J Neurophysiol 46:1177–1192.

Jones EG, Wise SP and Coulter JD (1979) Differential thalamic Relationships of sensory-motor and parietal cortical fields in monkeys. J Comp Neur 183:833–882.

Karnath HO, Fruhmann BM, Kuker W, Rorden C (2004): The anatomy of spatial neglect based on voxelwise statistical analysis: A study of 140 patients. Cereb Cortex 14:1164–1172.

Karnath HO, Ferber S, Himmelbach M (2001): Spatial awareness is a function of the temporal not the posterior parietal lobe. Nature 411:950–953.

Karnath HO, Zopf R, Johannsen L, Fruhmann Berger M, Nagele T, Klose U (2005): Normalized perfusion MRI to identify common areas of dysfunction: patients with basal ganglia neglect. Brain 128:2462–2469.

Mazziotta J, Toga A, Evans A, Fox P, Lancaster J, Zilles K, Woods R, Paus T, Simpson G, Pike B, Holmes C, Collins L, Thompson P, MacDonald D, Iacoboni M, Schormann T, Amunts K, Palomero-Gallagher N, Geyer S, Parsons L, Narr K, Kabani N, Le Goualher G, Boomsma D, Cannon T, Kawashima R, Mazoyer B (2001): A probabilistic atlas and reference system for the human brain: International Consortium for Brain Mapping (ICBM). Philos Trans R Soc Lond B Biol.Sci 356:1293–1322.

Mesulam MM (1998): From sensation to cognition. Brain 121:1013–1052.

Molenberghs P, Mesulam MM, Peeters R, Vanderberghe RR (2007): Remapping attentional priorities: differential contribution of superior parietal lobule and intraparietal sulcus. Cereb Cortex 17:2703–2712.

Morley JW, Goodwin AW, Darian-Smith I (1983): Tactile discrimination of gratings. Exp Brain Res 49:291–299.

Mort DJ, Malhotra P, Mannan SK, Pambakian A, Kennard C, Husain M (2004): Reply to: Using SPM normalization for lesion analysis in spatial neglect. Brain 127:E11.

Mort DJ, Malhotra P, Mannan SK, Rorden C, Pambakian A, Kennard C, Husain M (2003): The anatomy of visual neglect. Brain 126:1986–1997.

O'sullivan BT, Roland PE, Kawashima R (1994): A PET study of somatosensory discrimination in man. Microgeometry versus macrogeometry. Eur J Neurosci 6:137–148.

Oldfield RC (1971): The assessment and analysis of handedness: The Edinburgh inventory. Neuropsychologia 9:97–113.

Qureshi AI, Luft AR, Sharma M, Guterman LR, Hopkins LN (2000): Prevention and treatment of thromboembolic and ischemic complications associated with endovascular procedures: Part II–Clinical aspects and recommendations. Neurosurgery 46:1360–1375.

Reed CL, Caselli RJ, Farah MJ (1996): Tactile agnosia. Underlying impairment and implications for normal tactile object recognition. Brain 119:875–888.

Roland PE, Mortensen E (1987): Somatosensory detection of microgeometry, macrogeometry and kinesthesia in man. Brain Res 434:1–42.

Roland PE, O'sullivan B, Kawashima R (1998): Shape and roughness activate different somatosensory areas in the human brain. Proc Natl Acad Sci USA 95:3295–3300.

Rorden C, Karnath HO (2004): Using human brain lesions to infer function: A relic from a past era in the fMRI age? Nat Rev Neurosci 5:812–819.

Sakata H, Taira M, Murata A, Mine S (1995): Neural mechanisms of visual guidance of hand action in the parietal cortex of the monkey. Cereb Cortex. 5:429–438.

Sakata H, Takaoka Y, Kawarasaki A, Shibutani H (1973): Somatosensory properties of neurons in the superior parietal cortex (area 5) of the rhesus monkey. Brain Res 64:85–102.

Sathian K (1989): Tactile sensing of surface features. Trends Neurosci 12:513–519.

Schleicher A, Amunts K, Geyer S, Morosan P, Zilles K (1999): Observer-independent method for microstructural parcellation of

cerebral cortex: A quantitative approach to cytoarchitectonics. Neuroimage 9:165–177.

Schormann T, Zilles K (1998): Three-dimensional linear and nonlinear transformations: An integration of light microscopical and MRI data. Hum Brain Mapp 6:339–347.

Stoeckel MC, Weder B, Binkofski F, Buccino G, Shah NJ, Seitz RJ (2003): A fronto-parietal circuit for tactile object discrimination: an event-related fMRI study. Neuroimage 19:1103–1114.

Stoeckel MC, Weder B, Binkofski Choi H.J., Amunts K, Pieperhoff P, Shah NJ, Seitz RJ (2004): Left and right superior parietal lobule in tactile object discrimination. Eur.J.Neurosci. 19:1067–1072.

Talairach J, Tournoux P (1988): Co-planar stereotaxic atlas of the human brain.3-dimensional proportional system. An Approach to Cerebral Imaging. Stuttgart: Thieme.

Teuber HL (1955): Physiological psychology. Ann Rev Psychol 6:267–295.

Weder B, Nienhusmeier M, Keel A, Leenders KL, Ludin HP (1998): Somatosensory discrimination of shape: Prediction of success in normal volunteers and parkinsonian patients. Exp Brain Res 120:104–108.

Yousry TA, Schmid UD, Alkadhi H, Schmidt D, Peraud A, Buettner A, Winkler P (1997): Localization of the motor hand area to a knob on the precentral gyrus. A new landmark. Brain 120:141–157.

Zilles K, Schleicher A, Palomero-Gallagher N, Amunts K (2002): Quantitative analysis of cyto- and receptor architecture of the human brain. In: Mazziotta J Toga A, editors. Brain Mapping, the Methods. Amsterdam: Elsevier. pp 573–602.